Automated Hybrid TACT® Volume Reconstructions

N. I. Linnenbrügger[1, 2], R. L. Webber[3], L. P. Kobbelt[4], T. M. Lehmann[1]
[1]Department of Medical Informatics, Aachen University of Technology (RWTH), Aachen, Germany
[2]Department of Biomedical Engineering, Wake Forest University School of Medicine, Winston-Salem, NC, USA
[3]Departments of Dentistry and Biomedical Engineering, Wake Forest University School of Medicine, Winston-Salem, NC, USA
[4]Computer Graphics Group, Aachen University of Technology (RWTH), Aachen, Germany

Summary
Objectives: To design, implement in Java™, and evaluate a method and means for the automated localization of artificial landmarks in optical images for tuned-aperture computed tomography® (TACT®) that allows the replacement of radiographic with optical landmarks.
Methods: Circular, colored, optical landmarks were designed to provide flexibility with regard to landmark constellation, imaging equipment, and lighting conditions. The landmark detection was based on Hough transforms (HT) for ellipses and lines. The HT for ellipses was extended to enable selective detection of bright ellipses on a dark background and vice versa, and the number of irrelevant votes in the accumulator arrays was reduced. An experiment was performed *in vitro* to test the automated landmark localization scheme, verify registration accuracy, and measure the required computation time.
Results: A visual evaluation of the tomographic slices that were produced using the new method revealed good registration accuracy. A comparison to tomographic slices similarly produced by means of conventional TACT showed identical results. The algorithm ran sufficiently fast on standard hardware to allow landmark localization in "real time" during successive image acquisition in clinical applications.
Conclusions: The proposed method provides robust automated localization of landmarks in optical images. Using a hybrid imaging system, TACT can now be clinically applied without manual interaction of a human operator and without radiopaque landmarks, which might cover anatomic details of diagnostic interest.

Keywords
Computer-assisted image processing, X-ray computed tomography, three-dimensional imaging

Methods Inf Med 2004; 43: 315–9

1. Introduction

Tuned-aperture computed tomography® (TACT®) produces radiographic volume reconstructions using multiple planar radiographs acquired from various X-ray source positions. TACT is based on tomosynthesis [1] and extends as well as completely generalizes it. Other three-dimensional imaging modalities such as conventional tomography, tomosynthesis, and computed tomography require complete knowledge of the projection geometry prior to exposure. TACT differs from these modalities by circumventing this fundamental prerequisite. This is accomplished retrospectively by using information associated with the object of interest itself and its relationship to the X-ray detector [2]. Radiopaque spheres are usually attached as landmarks to the object of interest, and their images are manually localized in individual radiographic projections. The superior quality of TACT imaging in medical diagnostics has been reported in various clinical studies, especially in the fields of dentistry (e.g., [3, 4]), mammography (e.g., [5]), and nuclear medicine (e.g., [6]).

The main disadvantages of TACT are the time-consuming manual localization of the radiopaque landmarks and their obscuration of anatomic details, which reduces the quality of volume reconstructions. However, radiopaque landmarks can be replaced by optical (radiolucent) markers if a hybrid imaging system that combines a radiographic system with an optical camera is used [7]. This novel concept is referred to as *Hybrid TACT* and has not yet been formally published. Under certain geometric constraints, landmark positions observed in images acquired by a digital camera can be superimposed on concurrently acquired radiographic projections to produce tomographic slices. Appropriate normalization is possible using four additional landmarks and allows correction of projective artifacts produced when the optical and radiographic imaging planes are not parallel.

It is expected that the geometric constraints required by Hybrid TACT can be eliminated by building a specialized device where the optical camera is integrated in the X-ray source such that the foci of both systems are identical. However, optical landmarks must be localized automatically to support applications in clinical routine.

The task of automated landmark localization is not new. Related research has been done in the field of computer vision, where landmarks are often used to determine the location and orientation of the camera relative to a world coordinate system [8]. Landmark tracking methods based only on vision are computationally demanding. To avoid a frequent use of costly search algorithms, spatiotemporal coherence of the camera's movement is often assumed (e.g., [9, 10]) or additional non-vision sensors are applied (e.g., [11]). In contrast, the system presented here demands analysis of uncorrelated images from a single camera because, in general, the camera's position changes abruptly and unpredictably between the photographs. Therefore, a novel method and means for the automated detection of optical landmarks that is reliable and robust for a variety of applications is developed in this paper.

2. Methods

2.1 Landmark Design

A circle is chosen as the basic form of optical landmarks because of its mathematical simplicity. Circles appear as ellipses when projected onto the camera's imaging plane. The projection of a circle's center does not, however, coincide with the center of the corresponding ellipse. Consequently, the circle's center is marked. The circle's interior region is divided into four quadrants, two of which are black and the other two are given a certain color (Fig. 1) because TACT requires landmarks of distinguishable types. Information required for white balancing is included to reduce sensitivity to changes in illumination by circumscribing the inner circle with a white ring delimited peripherally by a thin black line (Fig. 1). In addition, a calibration mechanism is defined that includes the number and colors of respective landmarks as well as an estimate of the size of projected circles [12]. Together, this provides flexibility with regard to the number of landmarks and their constellation, the imaging equipment, and lighting conditions.

2.2 Landmark Detection

A directed edge image is created using Canny's edge detector [13], and all edge points not belonging to a closed boundary are removed [12]. The localization of shapes in the directed edge image is based on the Hough transform (HT), which collects votes for parametrically described shapes in an *accumulator array* [14]. In the case of ellipses, the parameter space is five-dimensional. According to the approach of Guil and Zapata [15], the dimensionality is reduced by splitting the detection process into three subsequent steps of only one or two dimensions: detection of (i) the center, (ii) the orientation, and (iii) the axes lengths.

The left side of Figure 2 shows the construction of a line of votes for the detection of an ellipse's center [15]. A and B are points on the ellipse, M_{AB} lies halfway between, and T_{AB} is the intersection of the tangents at A and B. In [15], parameters of lines $\overline{T_{AB}M_{AB}}$ that pass through the center of the ellipse are determined and peaks are found using a focusing algorithm that performs a hierarchical convergence to the solution. This procedure is equivalent to incrementing the value of accumulator cells along lines of infinite length. Accordingly, points erroneously vote for ellipse centers far away from their position. This leads to spurious accumulator peaks, especially in large images with many edge points. In this work, accumulator cells are incremented along line segments that have the length of half the largest expected major diameter of an ellipse, which is known from calibration. A line segment lies on $\overline{T_{AB}M_{AB}}$, starts at M_{AB}, and extends in the direction away from T_{AB}. Assume that A and B are points belonging to the same ellipse. The midpoint M_{AB} is then located inside the ellipse because ellipses are convex shapes. Consequently, the center of the ellipse cannot be displaced from M_{AB} by more than half the length of the major axis (Fig. 2).

An optical landmark contains nested circles with different configurations of brightness levels (Fig. 1). Thus, the ellipse detection must distinguish between bright ellipses on a dark background and dark ellipses on a bright background. For this, the gradient direction at A and B as well as the position of A and B relative to the line $\overline{T_{AB}M_{AB}}$ are considered. The vector that points from M_{AB} to T_{AB} is defined by point subtraction:

$$\vec{v} := T_{AB} - M_{AB} \quad (1)$$

The gradient vectors at A and B are denoted by $\vec{g}_A$ and $\vec{g}_B$, respectively. The equations

$$A_I = A + s_1 \cdot \vec{g}_A = M_{AB} + s_2 \cdot \vec{v} \quad (2)$$

$$B_I = B + s_3 \cdot \vec{g}_B = M_{AB} + s_4 \cdot \vec{v} \quad (3)$$

are then solved for s_1 and s_3, where s_i ($i \in \{1, \ldots, 4\}$) are unknown scalars and A_I and B_I denote the intersections of the line $\overline{T_{AB}M_{AB}}$ and the elongated gradient vectors at A and B, respectively. This determines the position of the intersections A_I and B_I relative to A and B and the gradient vectors $\vec{g}_A$ and $\vec{g}_B$. For bright ellipses on a dark background, the line $\overline{T_{AB}M_{AB}}$ lies "behind" A and B relative to $\vec{g}_A$ and $\vec{g}_B$ (Fig. 2), and s_1 and s_3 are smaller than zero. For the opposite configuration, $\overline{T_{AB}M_{AB}}$ is located "in front of" A and B. In this case, the solutions for s_1 and s_3 are greater than zero. If s_1 and s_3 have different signs, A and B do not belong to the same

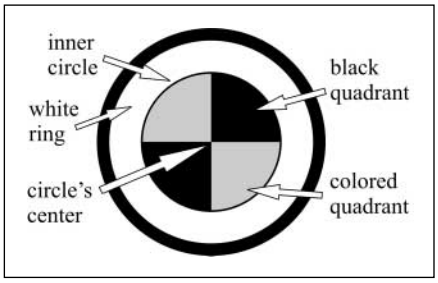

Fig. 1 Design of optical landmarks

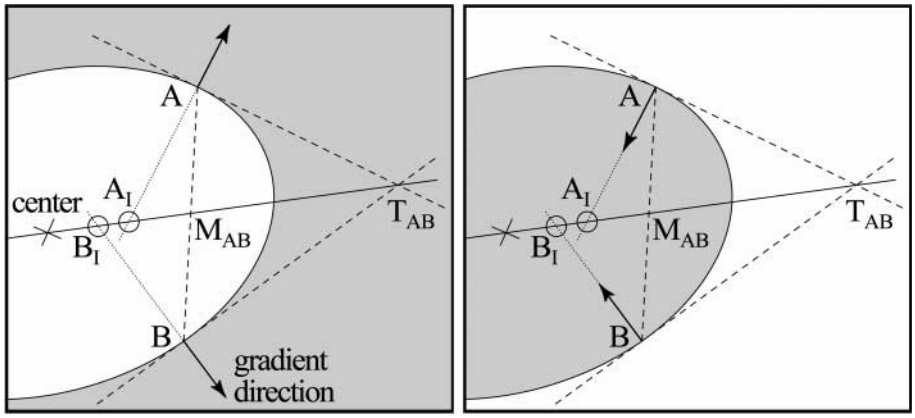

Fig. 2 Construction of a line of votes for the detection of an ellipse's center and distinction between bright ellipses on a dark background (left) and vice versa (right). A and B are points on the ellipse, M_{AB} lies halfway between, and T_{AB} is the intersection of the tangents at A and B. A_I and B_I denote the intersections of the line $\overline{T_{AB}M_{AB}}$ and the elongated gradient vectors at A and B, respectively.

ellipse and this pair of points is disregarded.

Complete bright ellipses on a dark background are identified as landmark candidates in the first detection stage. These correspond to the gradient between the white ring and the surrounding black border (Fig. 1). Subsequently, each candidate is further analyzed and segmented based on prior knowledge about the geometric structure of a landmark. Only the region within a candidate ellipse is considered, and a dark ellipse on a bright background is searched by means of another HT for ellipses. This ellipse corresponds to the gradient between the inner circle and the white ring (Fig. 1). Subsequently, two intersecting lines must be found inside the latter ellipse by means of the HT for lines. These lines together with the inner ellipse define the four quadrants of the landmark.

A landmark candidate is considered to be an actual landmark if all expected parts can be found and it fulfills certain homogeneity criteria for the inner circle quadrants and the white ring. Also, the degree to which the black quadrants are black and the white ring is white is taken into account. The assignment of found landmark candidates to landmarks is done according to the hue. The assignment can be verified because there must exist exactly one candidate for each expected landmark. The detection of landmarks is rejected if a bijective correspondence of detected and expected landmarks cannot be established. This stage uses distinct prior knowledge that is not used anywhere else in the detection process.

2.3 Experimental Evaluation

A cadaveric human jaw with teeth and soft tissues intact was examined. The specimen was fixed in the mouth of a head phantom (Fig. 3). An appropriate set of six optical landmarks was attached to the phantom, and two radiopaque spheres were fixed in front of the teeth to the soft tissues of the upper jawbone (Fig. 4). The X-ray source was a Siemens Heliodent (Siemens Medical Systems, Iselin, NJ, USA) operating at 60 kVp with 1.5 mm total aluminum equivalent filtration. The X-ray sensor was a CMOS[a] device (Schick Technologies, Long Island City, NJ, USA) with a total size of 640 × 900 pixels in *x*- and *y*-directions, respectively. It was placed behind the teeth in the mouth of the head phantom and fixed relative to the object. A digital camera (Olympus® CAMEDIA™ E-10) with a 4-million-pixel CCD[b] sensor was rigidly attached to the X-ray source.

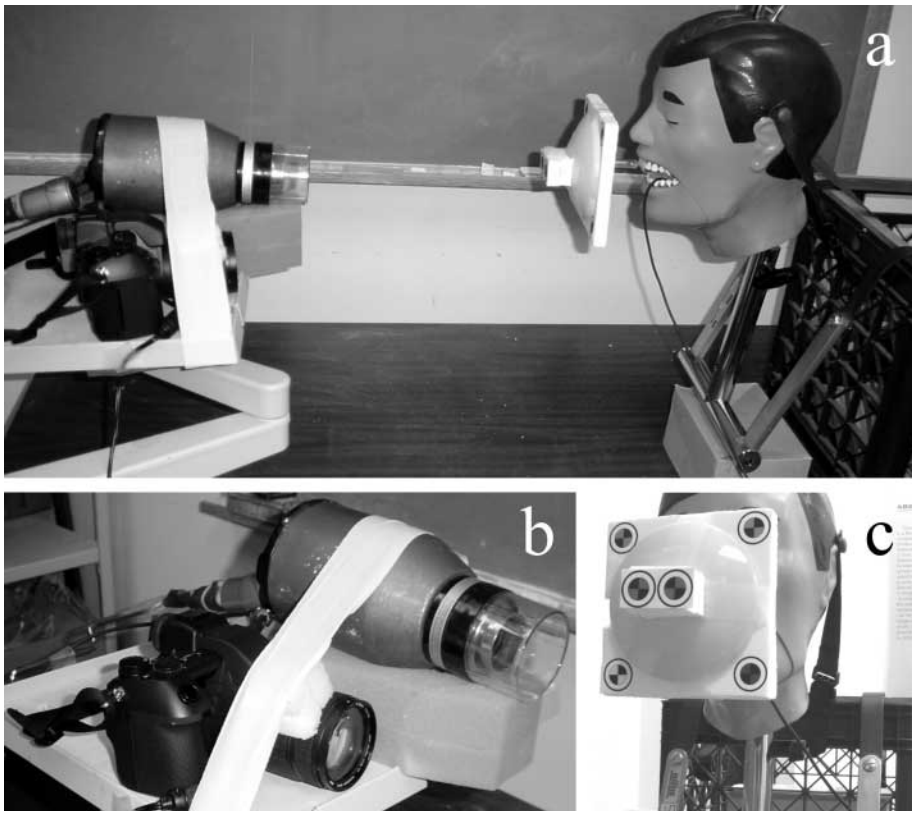

Fig. 3 Hybrid TACT experimental setup of X-ray source, photographic camera, and optical landmarks attached to the object: a) overview, b) coupled system of X-ray source and digital camera, and c) optically visible landmarks seen by the camera

The coupled X-ray source and photographic camera were placed on a horizontal platform that could be moved in space such that the platform remained horizontal. The platform was moved on a plane parallel to the X-ray sensor and positioned at 37 approximately evenly distributed locations. An X-ray projection as well as a photograph were acquired simultaneously at each position to produce corresponding series of radiographic and optical projections. The optical projections had a size of 1930 × 1644 pixels. Optical landmarks were detected in the optical projections using the automated landmark detection method, and the processing time was recorded. The landmark positions derived from the optical projections were used to produce tomographic slices *(hybrid reconstruction)*. Additionally, radiographic landmarks were manually localized in the plain radiographs and used for *conventional reconstruction*. Here, only 20 of 37 projections showed both landmarks. A total number of 51 equidistantly spaced tomographic slices extending over the entire specimen was produced using both reconstruction schemes.

[a] Complementary Mental Oxide Semiconductor
[b] Charged Coupled Device

3. Results

All six optical landmarks were detected successfully without any spurious responses in each of the 37 optical projections. This amounted to a total number of 222 detected landmarks. Initially, 479 ellipses were detected as landmark candidates. Almost all (256 of 257, i.e., 99.6%) of the falsely

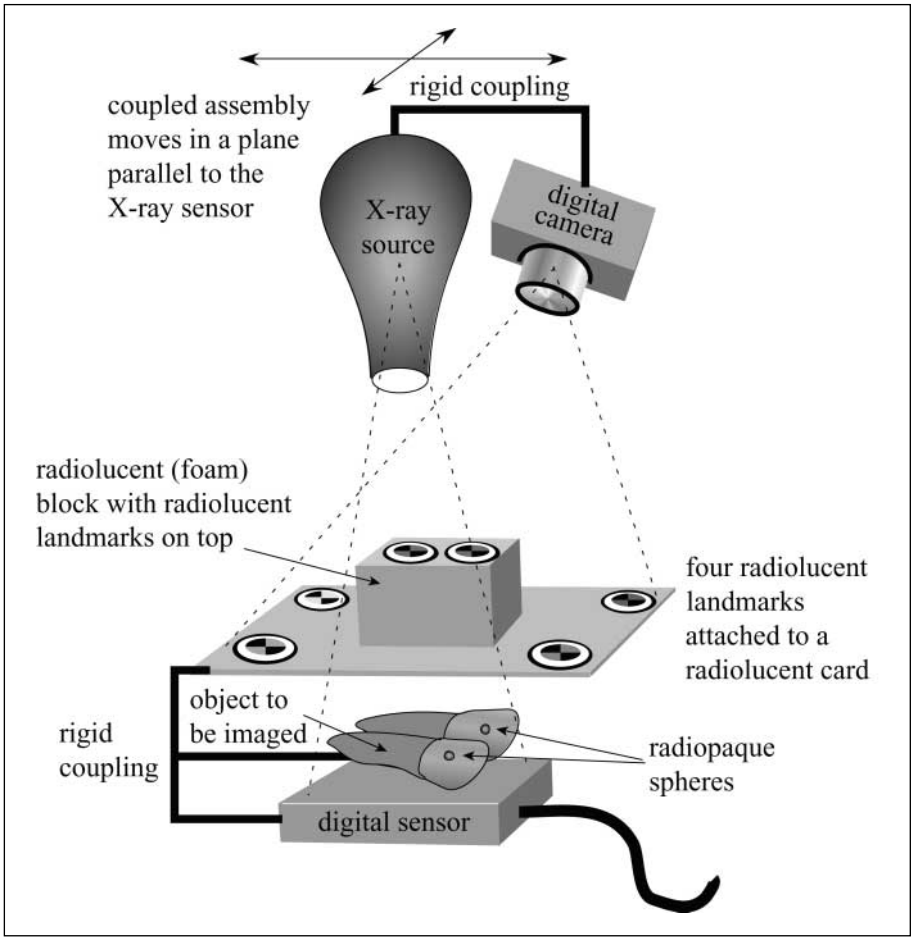

Fig. 4 Schematic illustration of the hybrid experimental setup used to image the central incisors of a cadaveric human jaw

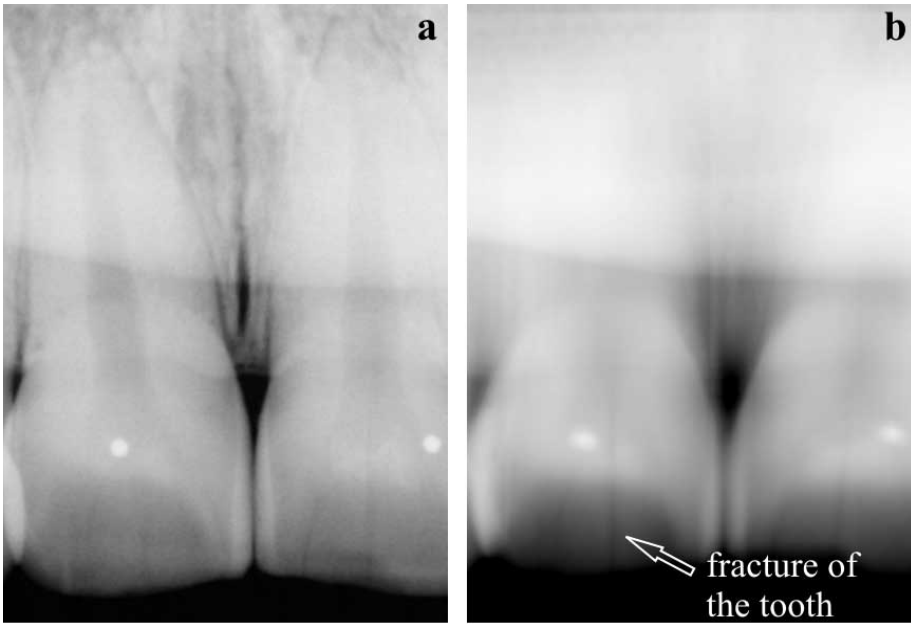

Fig. 5 Central incisors of a cadaveric human jaw: a) plane radiograph and b) reconstructed tomographic slice through a fracture of the tooth on the left (taken from the hybrid reconstructions series)

identified candidates were rejected in the next detection step that searched for dark ellipses on a bright background inside the candidate ellipses. The remaining false candidate was disregarded in the subsequent step because the localization of two intersecting lines within the ellipses (Fig. 1) failed. For all other candidates, it was successfully verified that detected landmark parts are homogeneous, and that there exists exactly one candidate for each expected landmark. The processing time was about 35.4 seconds per image using standard hardware (Intel® Pentium III-M, 933 MHz, 512 MB RAM) and the Java™ 2 Platform (Standard Edition, Version 1.3).

Figure 5a presents one of the original radiographs that were used to produce tomographic slices. Figure 5b shows the corresponding part of a tomographic slice through the fracture of the central incisor on the left (when viewed from above) that was taken from the hybrid reconstructions series. Note that the fracture is obvious in the tomographic slice, whereas it is invisible in the radiograph. This shows correct tomographic reconstruction by means of the automatically detected landmarks in optical images. The correctness of hybrid reconstruction was further verified comparing conventional with hybrid reconstructions, which appeared visually identical.

4. Discussion

We have introduced automatic image analysis to detect optical landmarks in photographs, which can be used for tomographic reconstruction. Landmark detection is based on the HT for ellipses. We have applied the algorithm of Guil and Zapata [15], which has been improved to provide better performance in images with many edge points and extended to selectively detect bright ellipses on a dark background and vice versa. These improvements are useful also for other applications of the HT for ellipses.

The landmark detection is performed in two stages: candidate detection and verification. The number and colors of landmarks, which are known from calibration,

are applied for the verification step. Nevertheless, most false candidates are rejected already in the candidate detection stage if essential components of landmarks cannot be found. Therefore, our approach of landmark design provides sufficient robustness for applications in clinical routine. Implemented in Java, the proposed algorithm runs on standard hardware in less than one minute per image. This is sufficiently fast to allow landmark extraction in "real time" during successive image acquisition in clinical applications.

The quality of TACT volume reconstructions depends on the accuracy of landmark localization. For conventional TACT, accuracy mainly depends on the ability of a human operator to specify the exact centers of projected landmarks. Contrarily, the accuracy of the automated detection system is determined by the intersection of two lines on a discrete grid, which can be computed with sub-pixel precision. A theoretical evaluation showed equal or better performance of the new approach for typical experimental setups as compared to conventional TACT [12]. Furthermore, accuracy of Hybrid TACT increases with the resolution of the digital camera in use. Depending on the quality of the camera's optical system, it may be necessary to correct for one or more inherent distortions.

In conclusion, Hybrid TACT allows the replacement of radiopaque by radiolucent landmarks and thereby eliminates tomographic blur. In this work, a new algorithm has been introduced that allows robust localization of optical landmarks for Hybrid TACT. The method is flexible with regard to different landmark constellations and digital cameras. Also, it is robust against variable lighting conditions. Therefore, TACT can now be used without manual interaction of a human operator in clinical applications.

References

1. Grant DG. Tomosynthesis: A three-dimensional radiographic imaging technique. IEEE Trans Biomed Eng 1972; 19: 20-8.
2. Webber RL, Horton RA, Tyndall DA, Ludlow JB. Tuned-aperture computed tomography (TACT™). Theory and application for three-dimensional dento-alveolar imaging. Dentomaxillofac Radiol 1997; 26: 53-62.
3. Chai-U-Dom O, Ludlow JB, Tyndall DA, Webber RL. Comparison of conventional and TACT® (tuned aperture computed tomography) digital subtraction radiography in detection of pericrestal bone-gain. J Periodont Res 2002; 37: 147-53.
4. Nance R, Tyndall D, Levin LG, Trope M. Identification of root canals in molars by tuned-aperture computed tomography. Int Endontic J 2000; 33: 392-6.
5. Suryanarayanan S, Karellas A, Vedantham S, Baker SP, Glick SJ, D'Orsi CJ, Webber RL. Evaluation of linear and nonlinear tomosynthetic reconstruction methods in digital mammography. Acad Radiol 2001; 8: 219-24.
6. Fahey FH, Grow KL, Webber RL, Harkness BA, Bayram E, Hemler PF. Emission tuned-aperture computed tomography: A novel approach to scintimammography. J Nucl Med 2001; 42: 1121-7.
7. Webber RL, Robinson SB, Fahey FH. Three-dimensional, tuned-aperture computed tomography reconstruction using hybrid imaging systems. In preparation. Correspondence to: Frederic H. Fahey, DSc, Division of Nuclear Medicine, Children's Hospital Boston, Boston, MA 02115, USA. E-mail: frederic.fahey@tch.harvard.edu; 2002.
8. Faugeras O. Three-Dimensional Computer Vision. Cambridge: MIT Press; 1993.
9. Jang G, Kim S, Lee W, Kweon I. Color landmark based self-localization for indoor mobile robots. In: Proceedings of the 2002 IEEE International Conference on Robotics and Automation (ICRA 2002); Piscataway: IEEE; 2002, pp. 1037-42.
10. Jiang B, You S, Neumann U. Camera tracking for augmented reality media. In: Proceedings of the 2000 IEEE International Conference on Multimedia and Expo (ICME 2000); Piscataway: IEEE; 2000, pp. 1637-40.
11. State A, Hirota G, Chen DT, Garrett WF, Livingston MA. Superior augmented reality registration by integrating landmark tracking and magnetic tracking. In: Rushmeier H (ed). SIGGRAPH 1996 Conference Proceedings. Reading: Addison Wesley 1996; pp. 429-38.
12. Linnenbrügger NI. Automated Hybrid TACT volume reconstructions using digital image processing. Master's Thesis, Department of Medical Informatics, Aachen University of Technology (RWTH), 52057 Aachen, Germany. E-mail: nilin@web.de; 2003.
13. Canny JF. A computational approach to edge detection. IEEE T Pattern Anal 1986; 8: 679-98.
14. Hough PVC. A method and means for recognizing complex pattern. US Patent Application No. 3069654, 1962.
15. Guil N, Zapata EL. Lower order circle and ellipse Hough transform. Pattern Recogn 1997; 30: 1729-44.

Correspondence to:
Thomas M. Lehmann
Department of Medical Informatics
Aachen University of Technology (RWTH)
52057 Aachen, Germany
E-mail: lehmann@computer.org